

Quantum Monte Carlo calculations of pion scattering from Li

T.-S. H. Lee and R.B. Wiringa

Physics Division, Argonne National Laboratory, Argonne, Illinois 60439

(October 24, 2018)

Abstract

We show that the neutron and proton transition densities predicted by recent Quantum Monte Carlo calculations for $A = 6, 7$ nuclei are consistent with pion scattering from ${}^6\text{Li}$ and ${}^7\text{Li}$ at energies near the Δ resonance. This has provided a microscopic understanding of the enhancement factors for quadrupole excitations, which were needed to describe pion inelastic scattering within the nuclear shell model of Cohen and Kurath.

PACS numbers: 21.60.Ka, 25.80.Ek

Quantum Monte Carlo (QMC) methods have been successfully developed to predict the properties of low-lying states of light nuclei starting with realistic two- and three-nucleon potentials [1]. While the reproduction of the energy spectra is the essential first step in such an effort, the dynamical content of the resulting nuclear wave functions must be tested against various reactions. This has been achieved so far mainly by considering electroweak processes [2,3]. In this paper we report on an additional test by using pion elastic and inelastic scattering.

Let us first briefly review the status of our understanding of pion inelastic scattering at medium energies ($80 \text{ MeV} < E_{\text{lab}} < 300 \text{ MeV}$). Because of the excitation of the Δ resonance, the pion-nucleus interactions in this energy region are dominated by the strong absorption mechanism. Consequently, the pion-nucleus inelastic scattering leading to discrete final nuclear states can be described by the Distorted Wave Impulse Approximation (DWIA). This has been well established [4–13] in very extensive investigations of the data from meson factories. Following the momentum-space approach [7], the inelastic scattering amplitude can be written as

$$T_{fi}(\vec{k}'_0, \vec{k}_0) = \int d\vec{k}' \int d\vec{k} \chi_{\vec{k}_0, f}^{(-)*}(\vec{k}') U_{fi}(\vec{k}', \vec{k}) \chi_{\vec{k}_0, i}^{(+)}(\vec{k}) , \quad (1)$$

where the \vec{k} 's are pion-nucleus relative momenta in the pion-nucleus center of mass frame, and the distorted waves $\chi^{(\pm)}$ are generated from an optical potential which is adjusted to fit the pion-nucleus elastic scattering.

The nuclear excitations are contained in the transition potential U_{fi} . It can be calculated from the πN scattering t-matrix and nuclear transition form factors. The details are given in Ref. [7]. To simplify the presentation, the spin-isospin variables will be suppressed here. Then the transition potential can be written as

$$U_{fi}(\vec{k}', \vec{k}) = t_{\pi n}(\vec{k}', \vec{k}, \omega_0) f_{fi}^{-1/2}(\vec{q}) + t_{\pi p}(\vec{k}', \vec{k}, \omega_0) f_{fi}^{1/2}(\vec{q}) , \quad (2)$$

where $\vec{q} = \vec{k}' - \vec{k}$, $t_{\pi n}(t_{\pi p})$ is an appropriately parameterized pion-neutron (pion-proton) scattering amplitude, and ω_0 is the collision energy calculated from using the fixed-scatterer approximation. With $t_3 = -1/2, 1/2$ denoting neutron and proton respectively, the nuclear transition form factors are defined by

$$f_{fi}^{t_3}(\vec{q}) = \int d\vec{r} e^{-i\vec{r}\cdot\vec{q}} \rho_{fi}^{t_3}(\vec{r}) , \quad (3)$$

with the transition densities defined by

$$\rho_{fi}^{t_3}(\vec{r}) = < \Psi_f | \frac{1}{A} \sum_{i=1,A} \delta(\vec{r} - \vec{r}_i) \frac{1 + 2t_3 \tau_z(i)}{2} | \Psi_i > , \quad (4)$$

where τ_z is the z-component of the nucleon isospin operator, and Ψ_i and Ψ_f are the initial and final nuclear states respectively. The transition dynamics can be better understood from the multipole expansion of transition densities

$$\rho_{fi}^{t_3}(\vec{r}) = \sum_{KM} \frac{1}{r^2} Y_{KM}(\hat{r}) < J_f M_f | J_i K M_i M > F_{K0,t_3}^{fiK}(r) , \quad (5)$$

Here we recall the notation of Ref. [7] to include possible spin transitions $S = 0, 1$ in $F_{KS,t_3}^{fiJ}(r)$, where K denotes the orbital angular momentum transition and $\vec{J} = \vec{K} + \vec{S}$ is the total angular momentum transfer.

In the DWIA study [7] for 1p-shell nuclei, the transition densities were calculated from the shell model of Cohen and Kurath [14]:

$$F_{KS,t_3}^{fiJ}(r) = \sum_{\alpha\beta} A_{J(KS)t_3}(\alpha, \beta; fi) (4\pi j_\alpha)^{1/2} \langle (l_\alpha 1/2) j_\alpha \parallel [Y_K(\hat{r}) \times \sigma_S]_J \parallel (l_\beta 1/2) j_\beta \rangle \\ \times R_{n_\alpha l_\alpha}(r) R_{n_\beta l_\beta}(r) \quad (6)$$

with $\sigma_0 = 1$, $\sigma_1 = \vec{\sigma}$, and

$$A_{J(KS)t_3}(\alpha, \beta; fi) = \langle \Psi_f \parallel [b_{\alpha t_3}^\dagger \times h_{\beta t_3}^\dagger]_{J[KS]} \parallel \Psi_i \rangle, \quad (7)$$

where $\alpha(n_\alpha, l_\alpha, j_\alpha)$ denotes the single particle orbitals, $R_\alpha(r)$ is the radial wave function, and b_α^\dagger and h_β^\dagger are the creation operators for the particle and hole states respectively.

It was found that the pion inelastic scattering from 1p-shell nuclei can be described by using the above shell-model input only when the quadrupole excitation component $J(KS) = 2(20)$ is enhanced by a factor $E_N \sim 2$. In Ref. [7], these enhancement factors were estimated from a systematic analysis of $B(E2)$ transitions from 1p-shell nuclei. For proton excitation, this enhancement factor is consistent with what is needed for explaining $B(E2)$ values. For $Z = N$ nuclei, one can assume that the neutron excitation also has the same enhancement because of isospin invariance. However, for the $N \neq Z$ nuclei, such as ^7Li , the enhancement factors for neutron excitations can not be obtained without making some additional assumptions. The predicted pion inelastic cross sections thus are not well justified theoretically. Furthermore, it would be desirable if the calculations do not include any enhancement factors. This however is very difficult, if not impossible, in practice within the shell model since the collective quadrupole excitations can only be described by a very large model space.

In this work, we calculate the transition densities for a given multipolarity by using wave functions from the recent QMC calculations for light nuclei. The input, Eq.(6), to the DWIA calculations for pion inelastic scattering is then defined by the following matrix element

$$F_{KS,t_3}^{fiJ}(r) = \frac{\langle \Psi_{J_f M_f} \mid \sum_{i=1,A} \delta(r - r_i) r_i^K [Y_K(\hat{r}_i) \times \sigma_S]_{JM} \frac{1+2t_3\tau(i)}{2} \mid \Psi_{J_i M_i} \rangle}{\langle J_f M_f \mid J_i J M_i M \rangle} \quad (8)$$

The QMC calculations use a realistic Hamiltonian containing the Argonne v_{18} two-nucleon [15] and Urbana IX [16] three-nucleon potentials, which we refer to as the AV18/UIX model. Both variational (VMC) and Green's function (GFMC) Monte Carlo calculations have been made for light nuclei [1]. The AV18/UIX model reproduces the experimental binding energies and charge radii of ^3H , ^3He , and ^4He , in the numerically exact GFMC calculations, but underbinds ^6Li and ^7Li by 2–5%. The variational Monte Carlo (VMC) energies are 2% above the GFMC results for $A = 3, 4$ nuclei and 10% above for $A = 6, 7$. However, the known excitation spectra are well reproduced by both the VMC and GFMC calculations, as are the charge radii. The VMC and GFMC calculations also produce very similar one-body densities, while two-nucleon density distributions differ by less than 10%.

The VMC wave functions have been used successfully to describe the elastic and transition electromagnetic form factors for ${}^6\text{Li}$ [2] without introducing effective charges. They have also given an excellent absolute prediction for the spectroscopic factors in ${}^7\text{Li}(e, e'p)$ reaction [3]. Consequently we expect the VMC wave functions to give a good estimate for both the elastic and transition densities required in pion scattering calculations.

The variational wave function for $A = 6, 7$ nuclei used here is the trial wave function, $|\Psi_T\rangle$, that serves as the starting point for the GFMC calculations. It has the general form

$$|\Psi_T\rangle = \left[1 + \sum_{i < j < k} \tilde{U}_{ijk}^{TNI} \right] \left[\mathcal{S} \prod_{i < j} (1 + U_{ij}) \right] |\Psi_J\rangle , \quad (9)$$

where U_{ij} and \tilde{U}_{ijk}^{TNI} are two- and three-body correlation operators and the Jastrow wave function $|\Psi_J\rangle$ is given by

$$|\Psi_J\rangle = \mathcal{A} \left\{ \prod_{i < j < k \leq 4} f_{ijk}^c \prod_{i < j \leq 4} f_{ss}(r_{ij}) \prod_{k \leq 4 < l \leq A} f_{sp}(r_{kl}) \right. \\ \left. \sum_{LS} \left(\beta_{LS[n]} \prod_{4 < l < m \leq A} f_{pp}^{LS[n]}(r_{lm}) |\Phi_A(LS[n]JMTT_3)_{1234:56...A}\rangle \right) \right\} . \quad (10)$$

The \mathcal{S} and \mathcal{A} are symmetrization and antisymmetrization operators, respectively. The central pair and triplet correlations $f_{xy}(r_{ij})$ and f_{ijk}^c are functions of relative positions only; the subscripts xy denote whether the particles are in the s- or p-shell. The $|\Phi_A(LS[n]JMTT_3)\rangle$ is a single-particle wave function with orbital angular momentum L , spin S , and spatial symmetry $[n]$ coupled to total angular momentum J , projection M , isospin T , and charge state T_3 :

$$|\Phi_A(LS[n]JMTT_3)_{1234:56...A}\rangle = |\Phi_\alpha(0000)_{1234} \prod_{4 < l \leq A} \phi_p^{LS}(R_{\alpha l}) \\ \left\{ \left[\prod_{4 < l \leq A} Y_{1m_l}(\Omega_{\alpha l}) \right]_{LM_L[n]} \times \left[\prod_{4 < l \leq A} \chi_l(\frac{1}{2}m_s) \right]_{SM_S} \right\}_{JM} \times \left[\prod_{4 < l \leq A} \nu_l(\frac{1}{2}t_3) \right]_{TT_3} . \quad (11)$$

Particles 1–4 are placed in an α core with only spin-isospin degrees of freedom, denoted by $\Phi_\alpha(0000)$, while particles 5–A are placed in p -wave orbitals $\phi_p^{LS}(R_{\alpha l})$ that are functions of the distance between the center of mass of the α core and particle l . Different amplitudes $\beta_{LS[n]}$ are mixed to obtain an optimal wave function by means of a small-basis diagonalization. For ${}^6\text{Li}$, the $(J^\pi; T) = (1^+; 0)$ ground state is predominantly a ${}^3\text{S}[2]$ amplitude, with small admixtures of ${}^3\text{D}[3]$ and ${}^1\text{P}[11]$ components, while the $(3^+; 0)$ first excited state is pure ${}^3\text{D}[3]$. For ${}^7\text{Li}$, the $(J^\pi; T) = (\frac{3}{2}^-; \frac{1}{2})$ ground and $(\frac{1}{2}^-; \frac{1}{2})$ first excited states are predominantly ${}^2\text{P}[3]$, with small admixtures of ${}^2,4\text{P}[21]$, ${}^2,4\text{D}[21]$, and ${}^2\text{S}[111]$ components. The $(J^\pi; T) = (\frac{7}{2}^-; \frac{1}{2})$ and $(\frac{5}{2}^-; \frac{1}{2})$ excited states are predominantly ${}^2\text{F}[3]$, again with small admixtures of ${}^2,4\text{P}[21]$ and ${}^2,4\text{D}[21]$ components. Mixing parameter values are given in Ref. [1].

The two-body correlation operator U_{ij} is defined as:

$$U_{ij} = \sum_{p=2,6} \left[\prod_{k \neq i,j} f_{ijk}^p(\mathbf{r}_{ik}, \mathbf{r}_{jk}) \right] u_p(r_{ij}) O_{ij}^p , \quad (12)$$

where the $O_{ij}^{p=2,6} = \boldsymbol{\tau}_i \cdot \boldsymbol{\tau}_j$, $\boldsymbol{\sigma}_i \cdot \boldsymbol{\sigma}_j$, $\boldsymbol{\sigma}_i \cdot \boldsymbol{\sigma}_j \boldsymbol{\tau}_i \cdot \boldsymbol{\tau}_j$, S_{ij} , and $S_{ij} \boldsymbol{\tau}_i \cdot \boldsymbol{\tau}_j$. The six radial functions $f_{ss}(r)$ and $u_{p=2,6}(r)$ are obtained from two-body Euler-Lagrange equations with variational parameters [17]. The f_{sp} and $f_{pp}^{LS[n]}$ correlations are similar to f_{ss} for small separations, but include parameterized long-range tails. The parameters used in constructing these two-body correlations, as well as the description of the three-body correlation operator \tilde{U}_{ijk}^{TNI} and the operator-independent three-body correlations f_{ijk}^c and f_{ijk}^p are given in Ref. [1].

In Ref. [7] it was found that inelastic transitions induced by pion scattering are dominated by the quadrupole transition $J(KS) = 2(20)$. In our QMC calculations, we evaluate the quadrupole transition density:

$$\rho_{E2}^{t_3}(r) = \frac{\sqrt{2J_f + 1} \langle \Psi_{J_f M_f} | \sum_{i=1,A} \delta(r - r_i) r_i^2 Y_2^M(\hat{r}_i) \frac{1+2t_3\tau(i)}{2} | \Psi_{J_i M_i} \rangle}{\langle J_f M_f | J_i 2M_i M \rangle}. \quad (13)$$

These neutron and proton transition densities are shown in Fig. 1 for four transitions in ${}^6\text{Li}$ and ${}^7\text{Li}$. The integrated $B(E2 \uparrow, t_3)$ values,

$$B(E2 \uparrow, t_3) = \frac{|\int \rho_{E2}^{t_3}(r) d^3r|^2}{2J_i + 1}, \quad (14)$$

are given in Table I, where they are compared to the experimental proton values obtained from (e, e') scattering and Coulomb excitation experiments [18–20]. Our evaluations are made with 160 000 Monte Carlo samples for transitions in ${}^6\text{Li}$ and 120 000 Monte Carlo samples for transitions in ${}^7\text{Li}$. This number of samples is sufficient to give statistical uncertainties that are as small or smaller than the errors on the experimental $B(E2)$ values. Other $J(KS)$ transition amplitudes can contribute to pion inelastic scattering, particularly in the ${}^6\text{Li}$ case, and are evaluated in a similar manner.

We see from Fig. 1 and Table I that the predicted differences between the neutron and proton excitations in ${}^7\text{Li}$ are very significant. Such differences can be most effectively verified by using an important characteristic of pion scattering at energies near the Δ excitation. At a typical energy $E_\pi = 164$ MeV, one finds that the πN amplitude in Eq.(2) has an interesting ratio $|t_{\pi^+ p}/t_{\pi^+ n}| = |t_{\pi^- n}/t_{\pi^- p}| \sim 3$. Consequently, the π^+ scattering is dominated by the proton excitations while π^- scattering is dominated by neutron excitations. The agreement with both the π^+ and π^- data will be a nontrivial test of the QMC wave functions. Thus the present study is complementary to that of Ref. [2] using electron scattering which mainly probes the proton excitations.

We first investigate pion scattering from ${}^6\text{Li}$. Here data for $E_\pi = 100, 180$ and 240 MeV [13] are available for testing the energy-dependence of our predictions. The pion optical potential and the πN t-matrix are taken from Ref. [7]. The πN amplitudes we employ are taken from the Karlsruhe-Helsinki analysis [21], and differ only slightly with the more recent VPI analysis [22], mainly in the S_{11} partial wave (as discussed in Ref. [23]). This partial wave and the other non- P_{33} partial waves are much weaker than the P_{33} channel in the energy region of interest near the Δ excitation. For the present exploratory investigation, we therefore do not make any effort to improve the optical potential employed in Ref. [7]. Such an improvement is probably needed in the future when the data at low energies and for the spin observables are investigated.

With transition densities calculated from QMC, there are no adjustable parameters in our DWIA calculations. In Table I, we see that the calculated $B(E2)$ for the transition to the

$(3^+, T = 0)$ state is in excellent agreement with the data. This is a significant improvement over the shell-model prediction which required a large enhancement factor $E_p = E_n = 2.5$ to reproduce the $B(E2)$ data, as discussed in Ref. [7]. We thus expect a similar improvement in pion scattering calculations.

Our results for ${}^6\text{Li}$ are displayed in Fig. 2. We see good agreement with the differential cross sections for elastic scattering. However, the discrepancies in reproducing the diffractive minima at 180 MeV indicate some deficiencies of the simple optical potential we have employed. We also see general agreement with the inelastic scattering to the $(3^+; T = 0)$ excited state, although some noticeable discrepancies are seen, particularly at 100 MeV. Nevertheless, it is fair to say that our results agree with the differential cross sections to a very large extent in both absolute magnitude and energy-dependence. The agreement seen in Fig. 2 is consistent with the $B(E2)$ values listed in Table I. The overall agreement is not surprising in view of the ability of the QMC wave functions to reproduce the elastic and transition form factors in electron scattering experiments [2]. To further improve the agreement with the data and to account for the spin observables, it would be necessary to improve the reaction model. For example, we may have to consider coupled-channel effects and refine the optical potential, but this is beyond the scope of the present investigation.

We next investigate the very old data for 164 MeV π^+ and π^- inelastic scattering from a ${}^7\text{Li}$ target [24]. The final states we consider are $(J^\pi; T) = (\frac{1}{2}^-; \frac{1}{2})$ at 0.478 MeV, $(\frac{7}{2}^-; \frac{1}{2})$ at 4.63 MeV, and $(\frac{5}{2}^-; \frac{1}{2})$ at 6.68 MeV. Our results are shown in Fig. 3. We see that the predicted cross sections (solid curves) are in excellent agreement with the data. In the same figure, we also show the contributions obtained using just the proton excitations. The agreement with both the π^+ and π^- data is evidently due to the delicate interplay between the neutron and proton excitations. If the shell model input given in Ref. [7] is used without the enhancement factors $E_n = 1.75$ and $E_p = 2.5$ for the quadrupole transition $J(KS) = 2(20)$, the predicted cross sections will be a factor of about 5 lower than the data for all of the cases considered here.

In conclusion, we have performed calculations of pion scattering from ${}^6\text{Li}$ and ${}^7\text{Li}$ using the nuclear transition densities predicted by the recent QMC calculations for light nuclei starting with realistic two-nucleon and three-nucleon potentials. The predicted cross sections are in very good agreement with the data. In contrast with the previous calculations using densities from nuclear shell model, the calculation does not include any enhancement factors. Because of the strong isospin dependence of the πN scattering t-matrix, the present investigation has probed critically the predicted neutron transition densities which are not well tested in electron scattering studies. Our results suggest that the wave functions predicted by the QMC calculations are accurate for investigating various nuclear reactions.

It is highly desirable to extend the present work to re-investigate the very extensive data of pion-nucleus scattering on larger 1p-shell targets and other more complex processes such as pion absorption and double-charge-exchange reactions. We expect that QMC wave functions for $A = 9, 10$ nuclei will become available in the next year. With the nuclear correlations correctly accounted for by using the wave functions predicted by QMC calculations, one now can hope to resolve many long-standing problems in intermediate-energy pion-nucleus reactions.

ACKNOWLEDGMENTS

We wish to thank D. Kurath and S. C. Pieper for many useful comments. Our work is supported by the U. S. Department of Energy, Nuclear Physics Division, under contract No. W-31-109-ENG-38.

REFERENCES

- [1] B. S. Pudliner, V. R. Pandharipande, J. Carlson, S. C. Pieper, and R. B. Wiringa, Phys. Rev. C **56**, 1720 (1997).
- [2] R. B. Wiringa and R. Schiavilla, Phys. Rev. Lett. **81**, 4317 (1998).
- [3] L. Lapikás, J. Wesseling and R. B. Wiringa, Phys. Rev. Lett. **82**, 4404 (1999).
- [4] H. K. Lee and H. McManus, Nucl. Phys. **A167**, 257 (1971).
- [5] G. W. Edward and E. Rost, Phys. Rev. Lett. **26**, 785 (1971).
- [6] T.-S. H. Lee and F. Tabakin, Nucl. Phys. **A226**, 253 (1974).
- [7] T.-S. H. Lee and D. Kurath, Phys. Rev. C **21**, 293 (1980); Phys. Rev. C **22**, 1670 (1980).
- [8] C. Olmer *et al.*, Phys. Rev. C **21**, 254 (1980).
- [9] S. J. Seestrom-Morris, D. Dehnhard, D. B. Holtkamp, and C. L. Morris, Phys. Rev. Lett. **46**, 1447 (1981).
- [10] S. J. Seestrom-Morris *et al.*, Phys. Rev. C **26**, 594 (1982).
- [11] C. L. Morris *et al.*, Phys. Rev. C **35**, 1388 (1987).
- [12] D. S. Oakley *et al.*, Phys. Rev. C **35**, 1392 (1987).
- [13] S. Ritt *et al.*, Phys. Rev. C **43**, 745 (1991).
- [14] S. Cohen and D. Kurath, Nucl. Phys. **73**, 1 (1965).
- [15] R. B. Wiringa, V. G. J. Stoks, and R. Schiavilla, Phys. Rev. C **51**, 38 (1995).
- [16] B. S. Pudliner, V. R. Pandharipande, J. Carlson, and R. B. Wiringa, Phys. Rev. Lett. **74**, 4396 (1995).
- [17] R. B. Wiringa, Phys. Rev. C **43**, 1585 (1991).
- [18] R. Yen, L. S. Cardman, D. Kalinsky, J. R. Legg, and C. K. Bockelman, Nucl. Phys. **A235**, 135 (1974).
- [19] W. J. Vermeer, R. H. Spear, and F. C. Barker, Nucl. Phys. **A500**, 212 (1989).
- [20] T. Lauritsen and F. Ajzenberg-Selove, Nucl. Phys. **78**, 1 (1966).
- [21] G. Höhler, F. Kaiser, R. Koch and E. Pietarinen, *Handbook of pion-nucleon scattering*, (Physics Data 12-1, Karlsruhe, 1979).
- [22] R. A. Arndt, I. I. Strakovsky, R. L. Workman, and M. M. Pavan, Phys. Rev. C **52**, 2120 (1995).
- [23] M. Batinić, I. Dadić, I. Šlaus, A. Švarc, B. M. K. Nefkens, and T.-S. H. Lee, Phys. Scripta **58**, 15 (1998).
- [24] J. Bolger, E. Boshitz, R. Mischke, A. Nagel, W. Saathoff, C. Wiedner, and J. Zichy, in *Meson-Nuclear Physics-1979*, Proceedings of the 2nd International Conference, Houston, Texas, edited by E. V. Hungerford III (AIP Conference Proceedings No. 54, New York, 1979).

TABLES

TABLE I. $B(E2 \uparrow, t_3)$ values in $e^2 \cdot \text{fm}^4$ for different transitions in ${}^6\text{Li}$ and ${}^7\text{Li}$. Experimental values are from Refs. [18,19]. Experimental uncertainties and Monte Carlo sampling errors are given.

${}^A\text{Z}(J_i \rightarrow J_f)$	Experiment		QMC
	p	p	n
${}^6\text{Li}(0^+ \rightarrow 3^+)$	21.8 ± 4.8	21.1 ± 0.4	21.1 ± 0.4
${}^7\text{Li}(\frac{3}{2}^- \rightarrow \frac{1}{2}^-)$	7.59 ± 0.10	5.7 ± 0.1	16.5 ± 0.3
${}^7\text{Li}(\frac{3}{2}^- \rightarrow \frac{7}{2}^-)$	15.5 ± 0.8	13.2 ± 0.2	34.6 ± 0.5
${}^7\text{Li}(\frac{3}{2}^- \rightarrow \frac{5}{2}^-)$	4.1 ± 2.0	2.3 ± 0.1	5.4 ± 0.2

FIGURES

FIG. 1. The transition densities, $\rho_{E2}^{n,p}$, for ${}^6\text{Li}$ and ${}^7\text{Li}$.

FIG. 2. Differential cross sections for ${}^6\text{Li}(\pi, \pi)$ and ${}^6\text{Li}(\pi, \pi')$ scattering at multiple pion energies. The data are taken from Ref. [13].

FIG. 3. Differential cross sections for ${}^7\text{Li}(\pi, \pi')$ scattering at $E_\pi = 164$ MeV. The data are taken from Ref. [24].

Fig. 1 Lee & Wiringa

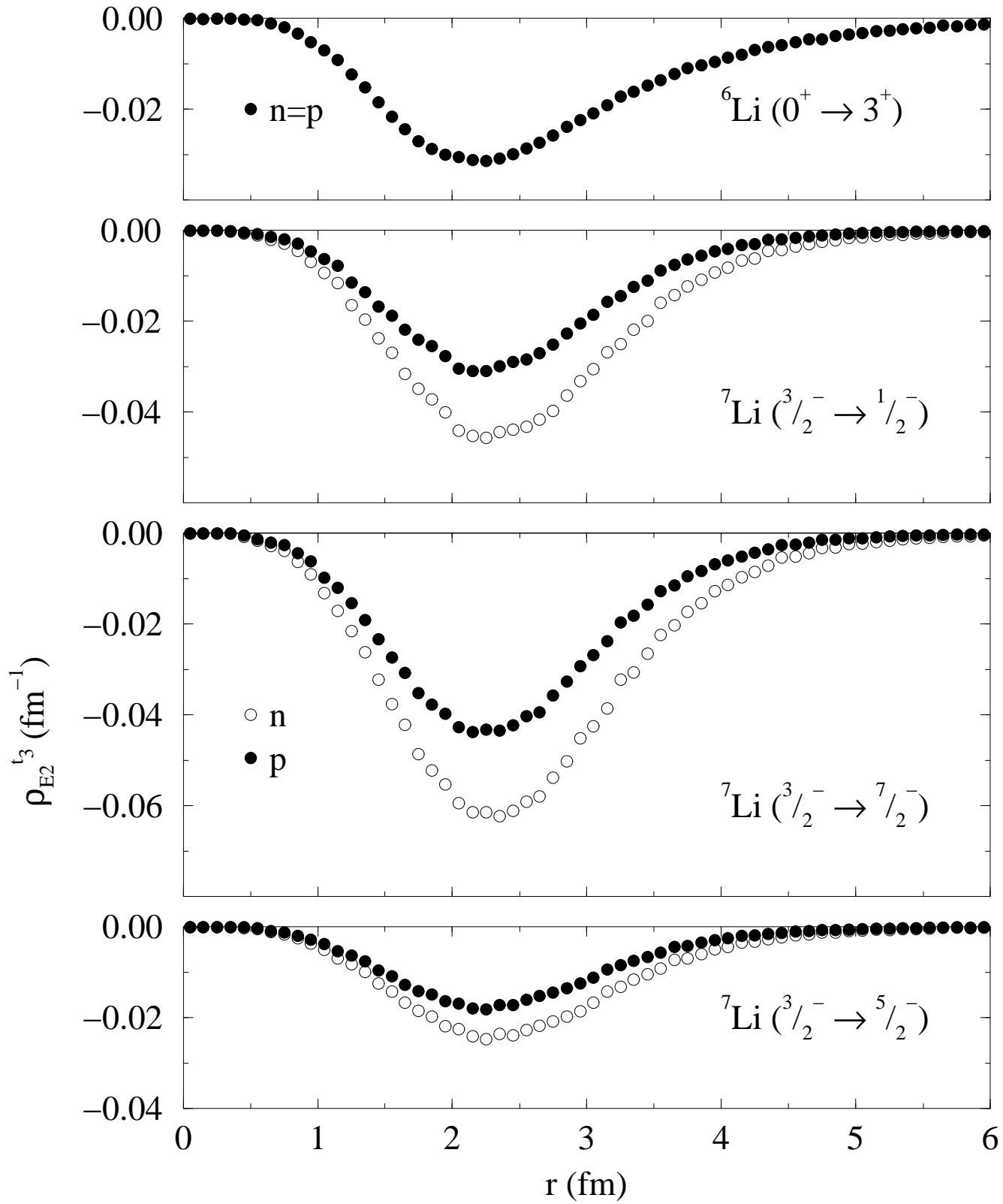


Fig. 2 Lee & Wiringa

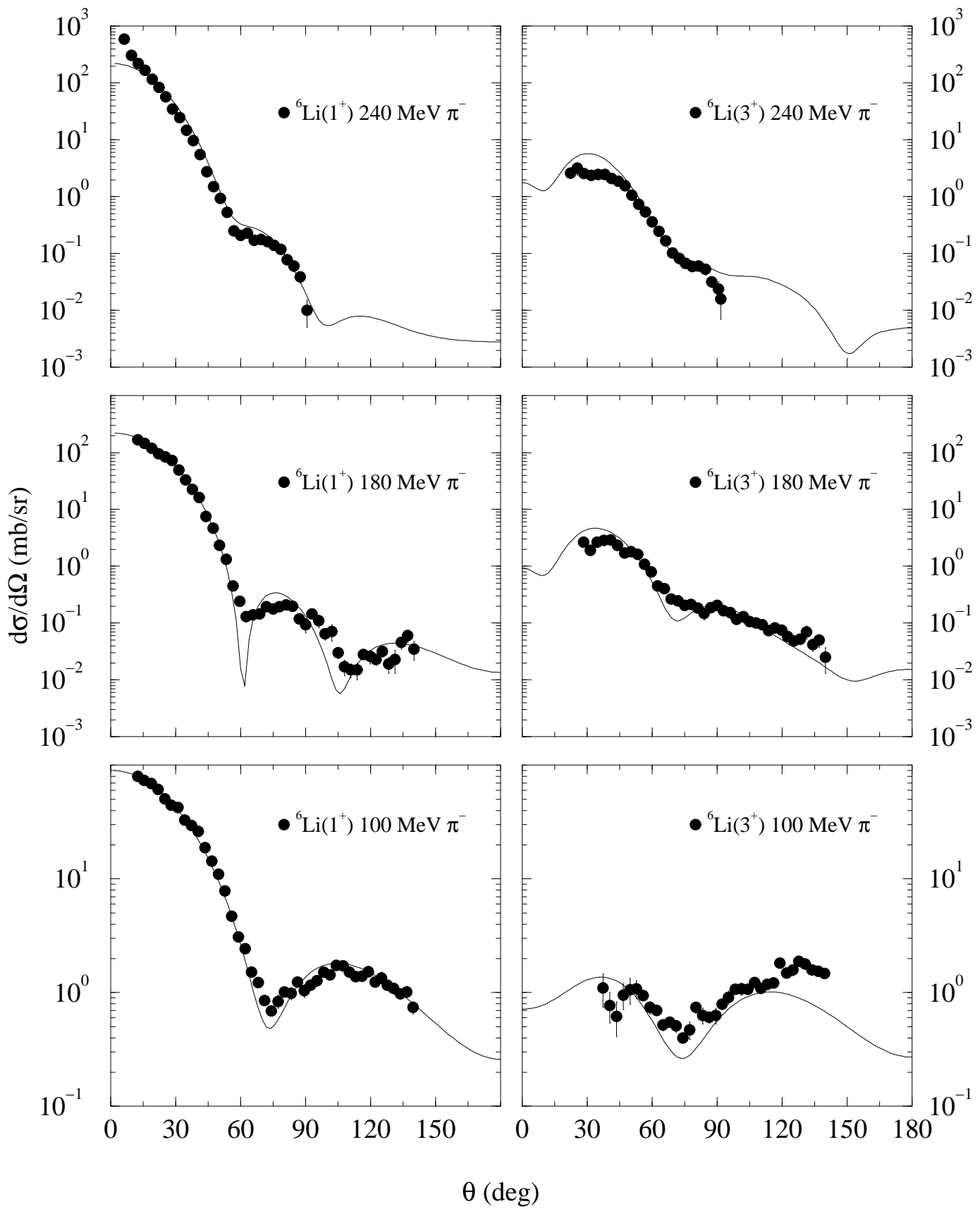


Fig. 3 Lee & Wiringa

